Interdot interactions and band gap changes in CdSe nanocrystal arrays at elevated pressure

Bosang S. Kim,[a] Mohammad A. Islam,[a] Louis E. Brus,[b] and Irving P. Herman[a),c)]
Materials Research Science and Engineering Center and the Columbia Radiation Laboratory, Columbia University, New York, New York 10027

(Received 5 October 2000; accepted for publication 8 March 2001)

Three-dimensional arrays of organically passivated CdSe nanocrystals were investigated under hydrostatic pressure using photoluminescence (PL) and absorption spectroscopies. Interdot separations were varied coarsely by varying the organic ligand on the nanocrystal and finely by applying hydrostatic pressure. The PL and absorption spectra of solutions and arrays of CdSe nanocrystals capped by either tri-n-octylphosphine oxide or tri-n-butylphosphine oxide are the same up to 60 kbar, which suggests that they exhibit no interdot coupling since the interdot separations in the solutions ($\sim$50 nm) are much greater than those in the arrays ($\lesssim$1 nm). While the variation with pressure is roughly that expected from the increase in band gap energy of bulk CdSe with pressure and the increase in confinement energies of electrons and holes with increased pressure, there is still a significant difference in the energy of the PL peak and the first exciton in absorption (the Stokes shift) for both these solutions and arrays that increases with pressure. This is attributed mostly to increased vibrational relaxation due to the movement of nuclei in the excited state. In contrast, there is a distinct difference between the pressure dependence of CdSe/pyridine dots in solution and arrays; the increase of the energy of the first exciton peak in absorption with pressure becomes markedly slower above about 30 kbar in CdSe/pyridine arrays, and is lower than that in the corresponding solution by $\sim$50 meV at 50 kbar and $\sim$70 meV at 60 kbar. Experiments with CdSe/shell/pyridine dots, with large electron and hole barriers, cast doubt on the mechanism of interdot electron and/or hole tunneling leading to a decrease in electron and/or hole confinement energy. Also, interdot tunneling of single carriers may be inhibited by the charge separation energy. The differences in the dielectric medium surrounding each dot in the solution and array explain their different absorption exciton energies at ambient pressure, but not the changes at elevated pressure. The observed loss of much of the pyridine ligands during array drying could be very significant, and contact between pyridine-capped dots at elevated pressure may be important. © *2001 American Institute of Physics.* [DOI: 10.1063/1.1369405]

I. INTRODUCTION

There is much interest in the properties of individual nanoparticles that are produced by the ''bottom-up'' growth approach. For example, the band gap of CdSe nanocrystals increases with decreasing nanocrystal size, leading to tunable linear optical properties.[1,2] Furthermore, such semiconductor quantum dots have generated interest as nonlinear optical materials because their oscillator strengths are concentrated in discrete highly polarizable excitonic states.[3] To enable efficient use of these structures, dense collections of these nanostructures can be assembled and used only if the properties of the individual dots are unaffected by their neighbors. This is one motivation for the study of dense collections of quantum dots. Another reason is precisely the interesting interactions that can occur and be controlled between neighboring dots.

Several types of site–site coupling have been observed in superlattices composed of both metallic and semiconductor dots. Collier *et al.*[4] have reported quantum coupling due to electron tunneling when they tuned the interdot spacing between organically passivated silver dots in two-dimensional arrays from 12 to 5 Å and observed a metal/insulator transition for an interparticle distance of $\sim$5 Å.[4–6] For semiconductor nanoparticles, Kagan *et al.* observed coupling between CdSe nanoparticles in close-packed three-dimensional (3D) arrays, which was attributed to classical dipole–dipole coupling described by Förster.[7,8] There appears to be little evidence of direct coupling of carriers between semiconductor nanoparticles, such as by tunneling, at ambient pressure. The photoconductivity experiments by Leatherdale *et al.*[9] suggest that the probability of charge separation in photoexcited CdSe quantum dot solids is small. A systematic transition from individual to collective, delocalized carrier states in clusters of CdSe nanoparticles was recently reported;[10] this is not consistent with what is reported here, possibly due to differing conditions.

In this article we search for evidence of interdot coupling by quantum mechanical tunneling between CdSe nanoparticles by comparing the near-band gap optical absorption and the photoluminescence (PL) of nanoparticle assemblies. This is done by comparing nanoparticles in dilute solution—

[a)]Also at: the Department of Applied Physics.
[b)]Also at: the Department of Chemistry.
[c)]Author to whom correspondence should be addressed; electronic mail: iph1@columbia.edu

 © 2001 American Institute of Physics

Downloaded 26 Jul 2002 to 128.59.115.125. Redistribution subject to AIP license or copyright, see http://ojps.aip.org/japo/japcr.jsp

where essentially no interdot coupling is expected—and in close-packed 3D arrays—where such coupling becomes more likely. The possibility of interdot coupling is examined as a function of distance between particles. Coarse tuning of the interdot separation is performed by varying the organic ligand that caps the dot. At ambient pressure, the interdot distance, measured from the outer surfaces of nearest-neighbor semiconductor nanocrystals is 11 ± 1 Å for tri-n-octylphosphine oxide (TOPO) capping molecules and 7 ± 1 Å for tri-n-butylphosphine oxide (TBPO) and pyridine capping molecules.[11,12] Fine tuning is provided by varying the applied hydrostatic pressure. For example, the interdot separation in CdSe/TBPO and CdSe/pyridine dot solids is ~5 Å or smaller at 70 kbar. The different capping molecules also lead to different electronic properties. TOPO and TBPO bond to surface Cd atoms via the lone electron pair on the oxygen atom, with zero formal charges on the O and P atoms. These ligands tend to confine the carriers within the nanoparticle core. Pyridine bonds to the Cd atoms via the lone pair of its nitrogen atom.[13] The resonance structure of the pyridine π ring is conducive to trapping holes, which may help transport of photoexcited holes from the semiconductor core of the dot for interdot coupling. Barriers to electron and/or hole transport can be constructed by analyzing arrays of CdSe dots (the core) overcoated with a shell layer of CdS, ZnSe, or ZnS.[14–16]

Interdot coupling of electrons and/or holes will lower the quantum confinement energy of each, which can be seen in photoluminescence and absorption (transmission) experiments if the coupling is sufficiently fast. Near a threshold pressure, interdot coupling may occur only in localized regions in an array, while at higher pressure it can occur throughout the sample. This decrease in band gap can be distinguished from the increase in band gap energy with pressure for these semiconductors by comparing the pressure dependence of the array with that of isolated dots in solution.

The absorption and PL probes provide qualitatively different information on different time scales. Absorption averages over the entire optical path in the beam, and reflects the electronic and nuclear structure that exists before instantaneous photon absorption; it is also much less sensitive to defects. The PL may come from localized regions, due to inhomogeneous quenching and/or exothermic energy transfer. Also, dephased PL on the nanosecond time scale reflects electronic structure after local dielectric and phonon relaxation, in response to the changed electrostatic properties in the excited electronic state. One consequence of interdot radiative transfer[7,8] is that excitation energy is transferred from smaller to larger nearby dots (with smaller confinement energy) and that it can be transferred to defect sites and be quenched before luminescence. Another difference is that PL can more sensitively sense the onset of interdot coupling at a pressure at which there may be only many scattered regions of localized coupling. This dispersed distribution of coupling would be a small component of the integrated absorption strength, but would be disproportionately large in PL because of radiative transfer from the smaller uncoupled dots (with larger carrier confinement energies) in the arrays to the larger coupled clusters of dots (with smaller confinement energies).

Quantum dot exciton PL in solution is generally Stokes shifted from the exciton peak observed in absorption.[17] This shift may be due to both electronic fine structure relaxation and vibrational (phonon) relaxation due to the movement of nuclei to new equilibrium positions in the excited state. (Deeper luminescence from defects, such as surface states, is also possible.) Modeling in Ref. 17 suggests that both effects occur in the PL of CdSe dots at 1 bar and room temperature, and are of comparable size. The vibrational Stokes shift is due to phonon motion along the LO phonon coordinate. It is difficult to directly observe this process, because the expected electronic and vibrational structure that should be present in the absorption and PL is masked by inhomogeneous (size distribution) broadening in most experiments. Our pressure studies provide a way to probe these effects in ensembles.

The Stokes shift also depends on the shape of the nanostructure,[17,18] so PL could be a sensitive indicator of band changes in tunnelling between any assembly of dots, including that between only two dots at the threshold of interdot coupling.

II. EXPERIMENTAL PROCEDURE

CdSe nanocrystals of ~3.3 nm diameter (5%–7% dispersion in radius) and passivated with TOPO were synthesized according to the method of Murray *et al.*[19] Core/shell nanoparticles were also prepared, with a CdSe core that was overcoated with a ~2-monolayer-thick CdS,[14,15] ZnSe,[16] or ZnS[15] shell, using the procedures described in the cited references. For each core/shell system the aim was to have approximately the same first exciton absorption peak energy in each case as for the ~3.3 nm diameter CdSe core-only dots. The core diameter/shell thickness/total diameter were respectively 2.0/0.7/3.4 nm for CdSe/CdS core/shell dots and 3.0/0.7/4.4 nm for both CdSe/ZnSe and CdSe/ZnS core/shell dots. The overcoating by CdS and ZnS was deemed to be successful and the PL intensities of both core/shell dots were very large as expected, even with the pyridine ligands; the overcoating by ZnSe was thought to be unsuccessful because of ZnSe dot nucleation and CdSe/ZnSe was not analyzed any further. In some experiments the TOPO/TOP cap on the surface of these CdSe/TOPO or CdSe/shell/TOPO particles was exchanged to leave either a TBPO, pyridine or 4-ethyl pyridine cap.[12,19] Table I lists the samples studied at elevated pressure.

Pyridine was chosen as a capping ligand because it is small and the resonant ring structure could help promote transport. The use of other small nitrogen-containing ligands was also considered. CdSe/butylamine was prepared but not examined at elevated pressure because the ligand binding was seen to be unstable (see later). Attempts to cap the dots by pyridazine (to increase the strength of ligand binding) and pyrazine (to link neighboring nanoparticles by the same molecule) were unsuccessful.

In the dilute solution runs, CdSe/TOPO dots were dispersed either in toluene or 4-ethyl pyridine and CdSe/

Downloaded 26 Jul 2002 to 128.59.115.125. Redistribution subject to AIP license or copyright, see http://ojps.aip.org/japo/japcr.jsp

TABLE I. Nanocrystals examined under pressure. All the arrays were loaded in liquid argon. The diameters are that of the semiconductor part of the dot; for core/shell nanocrystals, the diameters of the core and total core/shell dot are given.

Sample	Diameter (nm)	Data shown in Figs.
CdSe/TOPO solution in toluene or 4-ethyl pyridine	3.3	2
CdSe/TOPO array	3.3	2
CdSe/TBPO array	3.3	2
CdSe/CdS/TBPO array	2.0 (core), 3.4 (total)	1 and 2
CdSe/pyridine solution in 4-ethyl pyridine	3.3	4 and 5
CdSe/pyridine solution in MeOH/EtOH	3.3	5
CdSe/pyridine array	3.3	4 and 5
CdSe/CdS/pyridine array	2.0 (core), 3.4 (total)	6
CdSe/ZnS/pyridine array	3.0 (core), 4.4 (total)	6
CdSe/4-ethyl pyridine array	3.3	6

pyridine dots were dissolved in 4-ethyl pyridine or 80% methanol/20% ethanol mixtures and then loaded into the diamond anvil cell (DAC). 4-ethyl pyridine is a reasonable hydrostatic pressure medium up to at least 100 kbar[20,21] and the CdSe/pyridine nanoparticles are much more stable in it than in toulene;[22] it is also better than a methanol/ethanol mixture. Pyridine freezes at a low pressure (roughly at 10 kbar) and is an unsatisfactory loading medium. The possiblity of exchange of surface pyridine for 4-ethyl pyridine cannot be ignored, but it is not significant in evaluating these experiments since the particles are far apart in solution and the nature of the organic cap influences absorption little.[23] CdSe/pyridine is not highly stable in the methanol/ethanol mixture and the nanodots may clump a bit. Visual inspection suggested that there was no precipitation, so large clusters likely did not form. In these dilute solutions the interdot separation was roughly 50 nm.

Self-assembled close-packed amorphous arrays of dots were prepared directly on the top surface of one of the diamond anvils.[11,12] CdSe/TOPO, CdSe/TBPO, and CdSe/CdS/TBPO arrays were each prepared using a concentrated drop ($\sim$20% by weight) of the respective dots in 90% hexane/10% octane. All arrays of dots with pyridine or 4-ethyl pyridine caps were prepared by using the respective dots in solutions of pyridine or 4-ethyl pyridine. These drops spread radially and most of the solvent rapidly evaporates leaving visually transparent films that were approximately ~ 1 μm thick (which is roughly the absorption depth). These films were dried under vacuum for 1–2 h and then were stored under argon for 2–3 days; all of the solvent was removed very early during this procedure. Washing the dots during the size selection process[12,19] is important in removing excess capping groups form the dispersion; otherwise free TOP/TOPO crystallizes during the formation of the array.[24]

After the array was formed, the DAC was loaded with liquid argon to attain quasihydrostatic conditions. Organic and inorganic solvents commonly used to load samples into DACs were not used because they are known to swell the arrays, thereby increasing the interdot distance.[25] While the liquid argon may diffuse into the arrays into regions not occupied by the capping molecules, it will not appreciably affect the interdigitation of the capping molecules of nearest neighbor dots, and consequently the interdot distance. Visual inspection suggested that the arrays did not dissolve in the liquid argon.

Ruby chips were added during sample loading for pressure calibration measurements. Hydrostatic pressure was applied to these arrays in the DAC maintained at ambient temperature to control the interdot distance; reference measurements were also made on dilute solutions of these same dots for which the change in the $\sim$50 nm interdot distance is insignificant. At each pressure, most of these solutions and arrays were probed by both absorption spectroscopy (420–720 nm) and PL to study the band structure. PL was usually excited at 488 nm with an argon-ion laser; excitation at 325 nm with a He–Cd laser was performed to confirm that the PL spectra were independent of the excitation wavelength. PL was not used to probe CdSe/pyridine, because it has extremely weak PL,[19] or CdSe/TBPO arrays at ambient pressure, to avoid possible photo-oxidation by laser excitation before the DAC was sealed.

III. RESULTS

Figure 1 shows the PL and absorption spectra as a function of pressure for core/shell CdSe/CdS/TBPO arrays. These spectra are fairly typical for CdSe nanoparticles

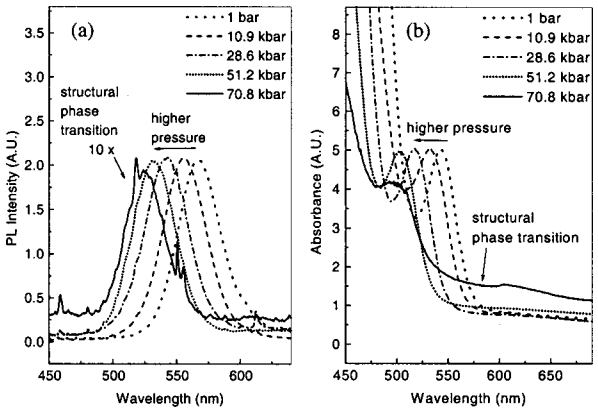

FIG. 1. (a) PL and (b) absorption spectra of CdSe/CdS/TBPO nanocrystal arrays as a function of pressure; for clarity only selected spectra at intermediate pressures are shown. These spectra are fairly typical for CdSe nanoparticles capped by TOPO or TBPO in dilute solution or in an array. Note the structural phase transition from wurtzite to rock salt above 65 kbar.

Downloaded 26 Jul 2002 to 128.59.115.125. Redistribution subject to AIP license or copyright, see http://ojps.aip.org/japo/japcr.jsp

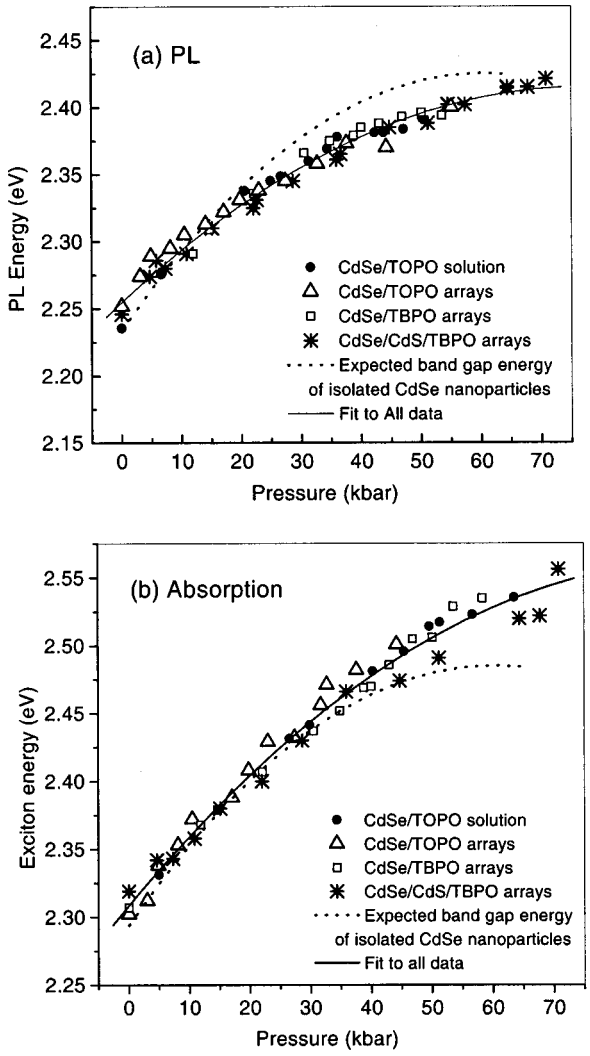

FIG. 2. (a) Peak energy of PL and (b) the first excitonic peak energy of the absorption spectra vs pressure for solutions and arrays of CdSe nanocrystals capped by either TOPO or TBPO. Each plot in each figure has been shifted vertically by up to ~10 meV so that each overlaps at 1 bar. The solid curve is a least squares to the data in each part. The expected band gap energy of isolated CdSe nanocrystals vs P is plotted in both parts, which accounts for changes in the bulk band gap and confinement energies.

capped by TOPO or TBPO that are in a dilute solution or an array. (For clarity, spectra are shown only at selected intermediate pressures. Spectral peak energies from all pressures are plotted in later figures.) Both series of spectra show the structural phase transition of CdSe to rock salt above 65 kbar in the upstroke.[20,21] In most cases, measurements were made after each pressure upstroke up to a value below that of this phase transition—to avoid the possibility of the hysteresis of the structural phase transition during the pressure downstroke—and then after each pressure downstroke. In these cases, data from the downstroke matched those from the upstroke. The energies of the peaks of the PL spectrum and the first excitonic peaks of the absorption spectrum of each sample at each pressure were determined by peak fitting. Figure 2(a) shows the peak energy of the photoluminescence versus pressure of CdSe/TOPO dispersed in dilute solution, CdSe/TOPO arrays, CdSe/TBPO arrays, and CdSe/CdS/TBPO arrays. Figure 2(b) shows the first excitonic

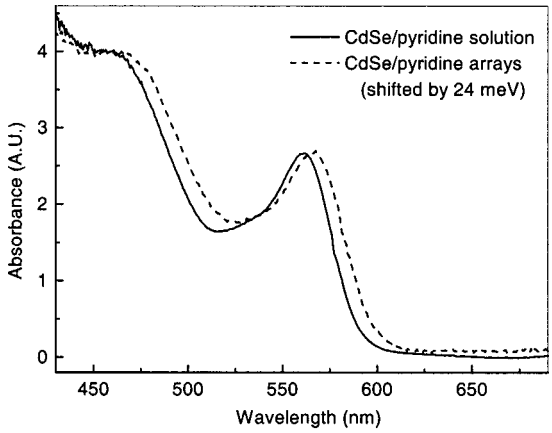

FIG. 3. Absorption spectra of CdSe/pyridine in solution and arrays at ambient pressure. The peak in the array is downshifted by 24 meV due to the change of the dielectric constant surrounding each nanoparticle.

energy of the absorption spectra versus pressure of the same systems. Each plot in each figure presented here and later has been shifted vertically in energy by a small constant amount (up to ~10 meV) so that each overlaps at 1 bar. These differences are due to the slightly different particle sizes in each run and, consequently, their slightly different confinement energies. The expected variation of band gap energy for isolated CdSe nanoparticles is also plotted. The most important contributions are the pressure dependences of the bulk CdSe band gap energy and of the electron and hole confinement energies. Both contributions increase with pressure; the band gap increase (~190 meV from 1 bar to 50 kbar) is much larger than that of the total confinement energy (~25 meV). (For CdSe/CdS nanocrystals, the presence of the CdS shell is not expected to perturb this pressure variation much.) In both parts of Fig. 2, the solid line is a fit of all data in that part. For each system the PL and absorption peaks both track the band gap of CdSe fairly well. There seems to be a divergence of the absorption and PL peaks with increasing pressure.

Figure 3 shows the absorption spectra of CdSe/pyridine in a dilute solution and CdSe/pyridine arrays at ambient pressure. The absorption peak in the array is redshifted. This is reproducible and is not attributable to oxidation, thermal effects, or instrumental errors. No redshift was seen in the absorption spectra of CdSe/TOPO arrays, confirming a previous report.[8]

Figure 4 shows typical absorption spectra of CdSe/pyridine in dilute solution and in arrays as a function of pressure. No PL was seen in either case, as was expected.[19] While the spectra for CdSe/pyridine in dilute solution vary with pressure the same way as those shown in Fig. 1, the spectra of the nanoparticles in arrays look qualitatively different. Above about 30 kbar the energy of the first excitonic peak increases much more slowly with increasing pressure than for the nanoparticles in solution (and it may actually decrease with pressure) and this peak broadens. Figure 5 plots the peak of the first excitonic peak in absorption for several CdSe/pyridine runs; the fit to the absorption peak data of Fig. 2 is also plotted. The pressure dependence of the peak in each CdSe/pyridine in solution run looks like those in Fig. 2, while that of each CdSe/pyridine array run looks

Downloaded 26 Jul 2002 to 128.59.115.125. Redistribution subject to AIP license or copyright, see http://ojps.aip.org/japo/japcr.jsp

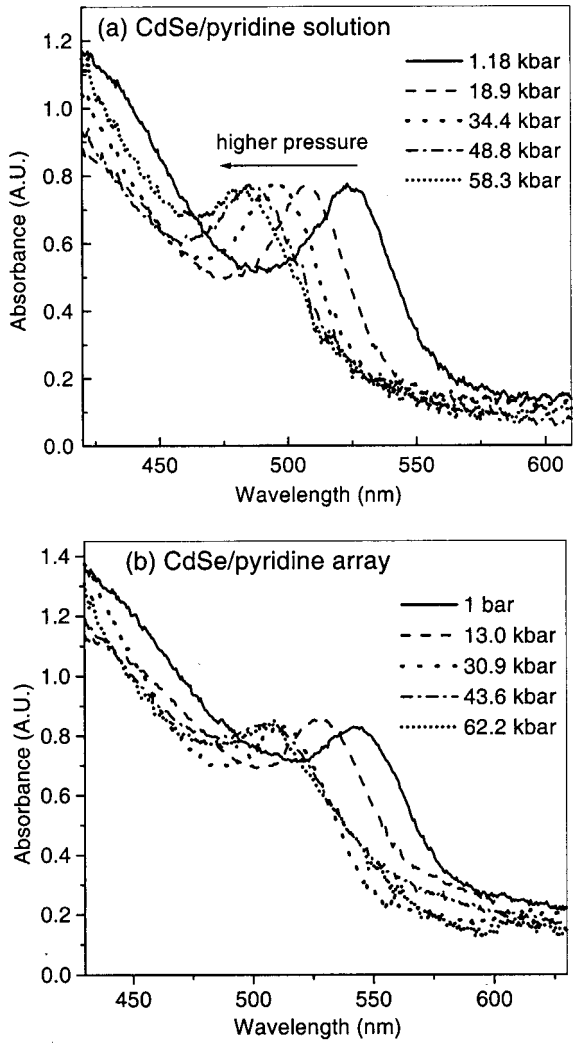

FIG. 4. Typical absorption spectra of CdSe/pyridine (a) in solution and (b) in an array as a function of pressure; for clarity only selected spectra at intermediate pressures are shown. Note that in (b) the spectrum at 43.6 kbar overlaps that at 62.2 kbar.

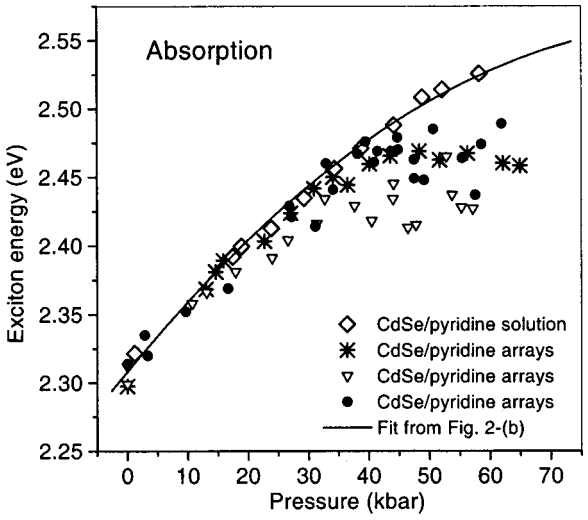

FIG. 5. The first excitonic peak energies in absorption spectra for several CdSe/pyridine runs. Note the significant difference between the solution and the array runs. Each plot has been shifted by up to ~10 meV so that each overlaps at 1 bar. The solid line is the fit to the exciton absorption data in (and also plotted in) Fig. 2(b).

very different. At 50 kbar the peak energy is ~50 meV lower than the reference curve from Fig. 2 and at 60 kbar it is ~70 meV lower.

The pressure dependences of related systems were also measured: CdSe/4-ethyl pyridine and the core/shell systems CdSe/CdS/pyridine, CdSe/ZnSe/pyridine, and CdSe/ZnS/pyridine. (Data for CdSe/CdS/TBPO dots were presented in Figs. 1 and 2.) For each of these dots in solution, the absorption—and for the cores/shell systems PL—spectra looked the same as for other dots in solutions in Figs. 2 and 5. The absorption and, when measurable, PL peaks of dried arrays of these nanoparticles are plotted versus pressure in Fig. 6, along with the respective data fits from Fig. 2. The PL data for core/shell/pyridine arrays look similar to those for TOPO and TBPO capped dots in Fig. 2. The absorption peak data look similar to those for CdSe/pyridine arrays in Fig. 5. The CdSe/pyridine in 80% methanol/20% ethanol solution run is also plotted in Fig. 6.

At times, spectra were taken several times at the same pressure. These spectra were the same, suggesting that these observations were not dependent on the history of incident light.

In one run the CdSe/TOPO array was heated to 80 °C for 1 h, and then examined at ambient temperature and elevated pressure. At ambient pressure there was the usual near-band gap PL peak as in Fig. 1, and a second weak broad PL peak at longer wavelengths. The wavelength of the near-band gap PL peak decreased with increasing pressure, as in Figs. 1 and 2; the center of the long-wavelength peak decreased from about 700 to 630 nm, and its intensity first increased greatly with pressure and then slowly decreased. These observations are qualitatively similar to those for CdSe particles in glasses examined at elevated pressure,[26] and are likely due to surface defects.

Absorption in CdSe/pyridine arrays prepared under different drying conditions was also examined as a function of pressure. Absorption at elevated pressure in arrays dried for short times, 1–2.5 h, looked similar to that for CdSe/pyridine solution and the ''standard'' runs in Fig. 2(b). Those arrays dried for 6 and 14 days exhibited the same large deviation from the absorption curve at elevated pressure as seen for the CdSe/pyridine arrays in Fig. 5. However, there was large hysteresis in the pressure downstroke, with exciton energies lower in the downstroke than the upstroke at the same pressure, which was not seen in the runs displayed in Fig. 5.

Attenuated total reflection (ATR) experiments in Fig. 7 show that pyridine does not bind very strongly to the dot, as is discussed later; capping by butylamine was seen to bind to CdSe nanoparticles even more weakly than does pyridine.

IV. DISCUSSION

A. Overall observations

The band gap of CdSe nanoparticles E_g^{nano} can be related to that of bulk CdSe E_g approximately by[2]

Downloaded 26 Jul 2002 to 128.59.115.125. Redistribution subject to AIP license or copyright, see http://ojps.aip.org/japo/japcr.jsp

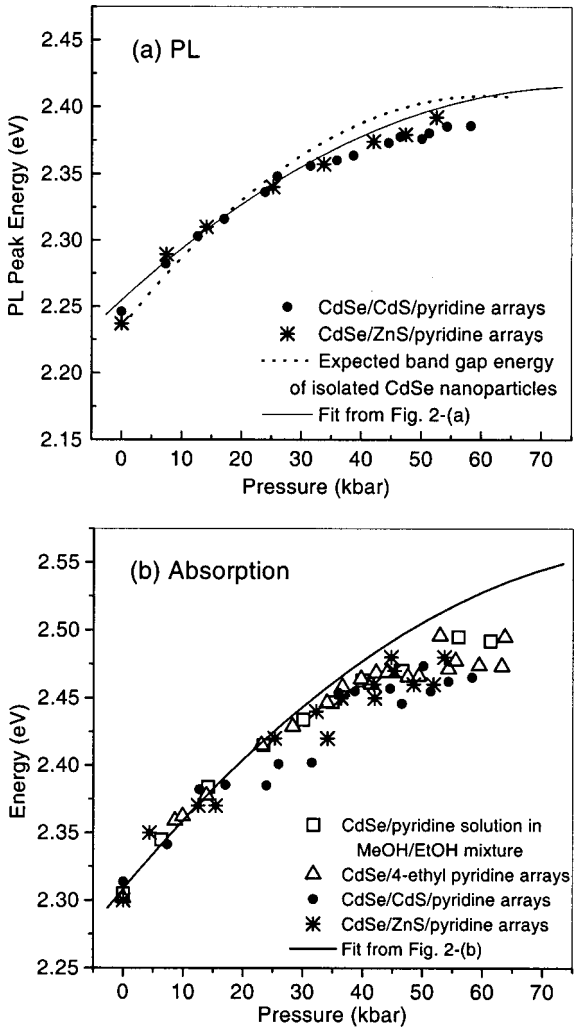

FIG. 6. (a) PL peak energies and (b) absorption peak energies of quantum dot arrays and solutions vs pressure for CdSe/shell/pyridine and CdSe/4-ethyl pyridine nanocrystals. Each plot in each figure has been shifted by up to ~10 meV so that each overlaps at 1 bar. The solid lines are the fits from the respective PL and absorption exciton energy data in Fig. 2. Note that the absorption peak energies in (b) are different from those in Fig. 2(b), while the PL peak energies in (a) are similar to those in Fig. 2(a).

$$E_g^{\text{nano}} = E_g + \frac{\hbar^2\pi^2}{2R^2}\left(\frac{1}{m_e}+\frac{1}{m_h}\right) - \frac{1.8e^2}{\epsilon_2 R} + \frac{e^2}{R}\overline{\sum_{n=1}^{\infty}\alpha_n\left(\frac{S}{R}\right)^{2n}} \tag{1}$$

with $\alpha_n=[(\epsilon-1)(n+1)]/[\epsilon_2(\epsilon n+n+1)]$. R is the radius of the nanoparticle, ϵ_2 is the dielectric constant of the nanoparticle, ϵ_1 is the dielectric constant of the surrounding medium, $\epsilon=\epsilon_2/\epsilon_1$, e is the elementary charge, and S is the magnitude of the distance that the wave function peaks from the center of the spherical particle.[2] The bar over the fourth term denotes an average over the wave function.[2] The second term in Eq. (1) is the quantum energy of localization for electrons of mass m_e and holes of mass m_h, the third term is the Coulomb attraction between electron and hole, and the fourth term is the dielectric solvation energy loss.[2] The band gap of bulk CdSe is 1.74 eV at 1 bar. The total confinement energy at ambient pressure is about 680 meV, of which 560 meV is from electron confinement and 120 meV is from hole confinement. The Coulomb attraction energy is −203 meV,

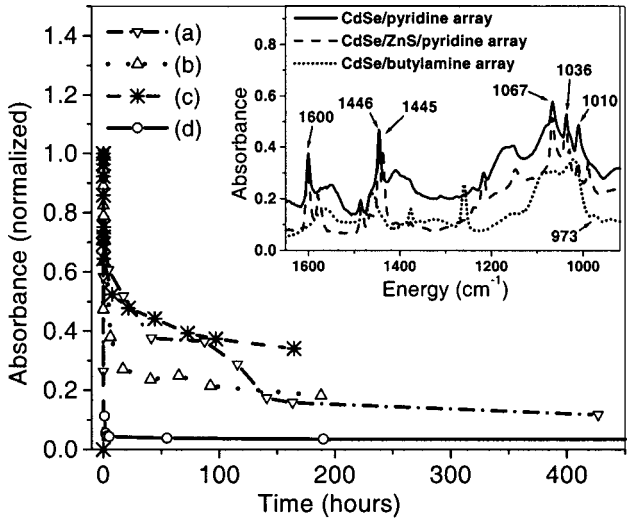

FIG. 7. Evolution of the height of ATR peaks during the drying of an array from nanoparticles in solution for (a), (b) the 1445 cm^{-1} bound pyridine peak for respectively CdSe/pyridine and CdSe/TOPO in pyridine solution, (c) the 1446 cm^{-1} bound pyridine peak for CdSe/ZnS/pyridine in pyridine solution, and (d) the 973 cm^{-1} bound butylamine peak for CdSe/butylamine in butylamine solution. Each trace is normalized to unity at the maximum, and represents the fraction of bound sites. The exchange of surface TOPO for pyridine is very fast in case (b). The inset shows the spectra for (a), (c), and (d), respectively, 20, 14, and 7 min into the drying. The 973 cm^{-1} butylamine peak has decayed greatly in 7 min. The peaks at 1010, 1036, 1067, and 1600 cm^{-1} are also due to pyridine bound to the CdSe dot.

and the last term due to the correction of the local dielectric constant is estimated to be +50 meV in a solution with $\epsilon=2.151$ (TOP). The last two terms represent the Coulomb attraction energy in the presence of the large dielectric discontinuity at the quantum dot surface. The net Coulomb energy is less than it would be in a CdSe macroscopic solid (term 3 only) because the dielectric solvation energy of the two charges decreases in the presence of the low dielectric constant capping molecules and solvent. As the charges are moving rapidly due to confinement energy in the dot, the high frequency, visible dielectric constants of CdSe and organics should be used in these terms. Equation (1) gives the energy of the absorption exciton peak; it does not include dielectric or phonon relaxation after photon absorption.

Each of the terms in Eq. (1) can vary with pressure P. The main variation with hydrostatic pressure is in the band gap energy of bulk CdSe E_g.[27] Using the characterization $E_g(P)=E_g(1\text{ bar})+\alpha P+\beta P^2$, the PL measurements of Ref. 27 on bulk CdSe found $\alpha=5.8\times10^{-3}$ eV/kbar and $\beta=-5.0\times10^{-5}$ eV/kbar^2 for measurements from 1 bar to the ~30 kbar phase transition pressure for bulk CdSe. Extrapolated to even higher pressure, this leads to increases by about the same 190 meV from 1 bar to 50 and 60 kbar. Next most important is the variation in confinement energy with the change in nanoparticle radius R with pressure. This is determined from the dependence of the volume V ($\propto R^3$) with P in Murnaghan's Equation $V(P)=V(1\text{ bar})[1+PB'/B]^{-1/B'}$, where B (=370 kbar for wurtzite CdSe)[21] is the bulk modulus and $B'=dB/dP$ (=11 for CdSe).[21] From 1 bar to 50 kbar R decreases by 3%, and the confinement energy increases by 25 meV assuming that the effective

Downloaded 26 Jul 2002 to 128.59.115.125. Redistribution subject to AIP license or copyright, see http://ojps.aip.org/japo/japcr.jsp

masses are constant. The dependences of the $m_{e,h}$ and ϵ on pressure are likely less important. (This is not certain; for example, the dependences in bulk InP are not insignificant.[28] Also, see later.) Consequently, the change in energy with P other than the band gap (confinement, exciton and solvation energy) is approximately equal to the measured change in band gap energy with change of radius at 1 bar. This variation of band gap energy with P is plotted in Fig. 2. All band gap changes except for those of arrays of nanoparticles capped by pyridine or 4-ethyl pyridine are quite reasonably modeled by this variation. The net Coulomb energy (terms 3 and 4) should increase as pressure increases, because as the CdSe and organics become more dense, the concentration of electrons and thus the visible dielectric constants will increase. As the compressibility of the organics is much higher than that of CdSe, the fractional increase in the organic dielectric constant might be larger than that of CdSe.

In each run with TOPO or TBPO capping molecules the pressure dependence of the first excitonic peak in absorption and the PL peak each was the same for the solution and array of the same type of nanoparticles (CdSe/TOPO, CdSe/CdS/TOPO, CdSe/TBPO), which suggests no observable carrier coupling between dots. In each case the variation with pressure is that expected from the increase in band gap energy of bulk CdSe with pressure and the increase in confinement energies of electrons and holes with increased pressure, which results from the smaller dot dimensions. Tracking with the expected gap looks better for the PL peaks than for absorption. However, this is not certain because of the extrapolation and the uncertainty in the α and β coefficients for bulk CdSe, which could be measured up to only about 30 kbar due to the structural phase transition in bulk CdSe.

These absorption and PL peaks varied differently with pressure, especially above 40 kbar (Fig. 2). From least-squares fit of all the data, the α and β coefficients for the PL peaks in Fig. 2(a) are $\alpha = 4.15 \pm 0.16 \times 10^{-3}$ eV/kbar and $\beta = -2.69 \pm 0.24 \times 10^{-5}$ eV/kbar^2, and those for the absorption peaks in Fig. 2(b) are $\alpha = 5.36 \pm 0.20 \times 10^{-3}$ eV/kbar and $\beta = -2.83 \pm 0.30 \times 10^{-5}$ eV/kbar^2. The Stokes shift between absorption and PL is seen to increase dramatically with pressure.

Since the pressure dependences of both PL and absorption were the same for the dilute solution and the arrays in these cases, the method of preparing the arrays directly on the diamond anvil apparently does not lead to nonhydrostatic stress conditions.

A distinct difference in the pressure dependence of the absorption spectra of arrays and solutions was seen only for CdSe nanocrystals capped by pyridine. The pressure dependence of the first excitonic absorption peak in isolated CdSe/pyridine looks the same as that in all runs of CdSe/TOPO and CdSe/TBPO. However, the exciton energy with pressure curve levels off for the CdSe/pyridine array; it is possible that it decreases with pressure. This was only observed in absorption since no PL could be observed from the pyridine-capped particles. At ambient pressure the confinement energies of electrons and holes in CdSe nanoparticles of 3.3 nm diameter are ~560 and 120 meV, respectively. At 60 kbar the absorption exciton peak in CdSe/pyridine in arrays dried for 3 days is lower than that in solution by ~70 meV, which is a significant fraction of the confinement energy of either carrier. The absorption energies at high pressures for CdSe/pyridine arrays are still larger than the PL energies seen in the other CdSe dot systems studied that luminesce.

The only run of CdSe/pyridine in solution whose results differed from all of the other solution runs (and the TOPO and TBPO array runs) was that in 80% methanol/20% ethanol solution (Fig. 6). Since CdSe/pyridine is not highly stable in this methanol/ethanol mixture, the nanodots may clump a bit, even with their pyridine caps. This may be an indication of localized interdot tunneling in solution.

B. Stokes shift

At ambient pressure the Stokes shift between absorption and PL is ~60 meV. It increases dramatically with pressure, by ~57 meV at 50 kbar. This large pressure-induced Stokes shift is seen for all samples that emit PL, i.e., dots capped by TOPO or TBPO and CdSe/shell/pyridine dots. This large increase in Stokes shift is seen in both dilute solutions and arrays, and is therefore unlikely due to nonhydrostatic effects (solutions and arrays are loaded in the diamond anvil cell differently) or contact between the nanocrystals. It is unlikely due to surface states since it is seen for both core-only and core/shell dots, and the interfaces critical for PL are very different in these two cases (core/organic ligand interface for core-only dots and core/shell interface for core/shell dots). It is likely due to ''bulk'' states.

Two possible contributions to the Stokes shift are: (1) a purely electronic shift due to the splitting of exciton states into ''bright'' and ''dark'' excitons (electronic Stokes shift) and (2) vibrational (phonon) relaxation due to movement of nuclei to new equilibrium positions in the excited state (vibrational Stokes shift). Each contribution can change with pressure. Reference 29 found good agreement between the theory of the nonresonant Stokes shift at ambient pressure with experiments by considering both contributions, ensemble averaged over the experimental and shape distributions of the dots.

The expected change in the purely electronic component of this nonresonant Stokes shift[30] with pressure is estimated considering the nanocrystal states for monodisperse and monoshaped 3.3 nm diameter dots using the theory presented in Ref. 30, without phonon corrections. Dots with ellipticity 0 (spherical), 0.28 (prolate), and −0.28 (oblate) are considered. The splitting of the highest strongly absorbing exciton state and the lowest exciton state (nonabsorbing) is calculated for pressure-induced changes in dot size and effective masses, and possible changes due to dot shape. This corresponds to the $0^U \leftrightarrow \pm 2$, $1^U \leftrightarrow 0^L$, and $0^U \leftrightarrow \pm 2$ splittings in the spherical, prolate, and oblate dots respectively, and 35.3, 29.6, and 76.8 meV Stokes shifts respectively at 1 bar. (Only the highest very strongly absorbing state is used, which slightly overestimates the shifts.)

Smaller dots with larger confinement energy have larger Stokes shifts.[30] As pressure is increased from 1 bar to 50 kbar, an increase in the Stokes shift of only 1.4 meV is expected for spherical dots (3.3 meV for prolate and 3.6 meV

Downloaded 26 Jul 2002 to 128.59.115.125. Redistribution subject to AIP license or copyright, see http://ojps.aip.org/japo/japcr.jsp

for oblate). The Stokes shift also depends on the ratio of the light and heavy hole effective masses m_{lh}/m_{hh} (0.28 at 1 bar for bulk CdSe).[29] The three-band Kane model is used to estimate this ratio at elevated P; it predicts that m_{hh} does not change with P and $dm_{lh}/dP = m_{lh}(\alpha/E_g^{\text{nano}})$.[31] From 1 bar to 50 kbar, m_{lh}/m_{hh} increases by a factor of 1.13, which causes the Stokes shift to increase by 0.8 meV for spherical dots (decrease by 2.8 meV for prolate and 0.9 meV for oblate). Collectively, the radius and effective mass effects increase the Stokes shifts respectively by 2.2, 0.4, and 2.6 meV for spherical, prolate, and oblate dots, which are much smaller than the $\sim$57 meV increase that is seen here. This assumes unchanging exciton radius, which depends on m_e/m_h. Assuming the increasing m_e/m_h with decreasing volume calculated for InP,[28] pressure-induced increases in the electronic Stokes shift would be smaller, and sometimes the shift would decrease with P.

A large increase in the purely electronic component of the Stokes shift, consistent with observations, would be predicted if the dots became progressively more oblate with pressure.[30] The x-ray diffraction studies of Ref. 32 report no change in dot shape with pressure, except at the phase transition between four-fold and six-fold coordination. The Stokes shift observations reported here could be consistent with very nonhydrostatic conditions, but such nonhydrostaticity is inconsistent with the observations of similar Stokes shift increases with P in solutions and arrays. Similarly, large increases in the electronic Stokes shift would be possible if PL were selectively quenched in more prolate dots at higher P; however, this would suggest a narrowing of the inhomogeneous PL spectrum at elevated P, which is not observed.

The change of the electronic Stokes shift with pressure is not expected to be large, and it appears that the increase in Stokes shift with pressure represents an increase in the vibrational (LO phonon) Stokes shift. It is difficult to model this because the strength of the coupling is not understood well at 1 bar, and appears to vary widely dot to dot in single nanocrystal studies. The coupling is very sensitive to wave function details in model calculations. It is unknown how it varies with pressure.

A third possibility for the Stokes shift should also be considered. Since the fractional compression of the capping molecules and solvent is large, the organics may be more strongly coupled to the nanocrystal exciton at $\sim$50 kbar, as they are squeezed into the nanocrystal surface, than at 1 bar. In this case the dielectric relaxation of the polar capping molecules may contribute to the Stokes shift; this type of effect is modeled in the Marcus theory of solvent relaxation around dissolved molecules.[33] Again it would be difficult to model this quantitatively.

C. Mechanisms for interdot interactions

1. Quantum mechanical interdot coupling

One possible explanation for this unusual observation in CdSe pyridine arrays might be rapid charge separation (hole or electron tunneling to a neighboring dot) or energy migration (both hole and electron) among dots, on the femtosecond time scale with interdot couplings of order 50 meV as apparently measured in absorption. These processes would have to occur before hole transfer to the pyridine ligand, which is known to occur in 0.5 ps for dissolved dots.[34] In the TOPO-coated dots, where the TOPO layers remain intact in the arrays, neither energy transfer nor charge separation is this fast. Also, charge separation by tunneling to a neighboring dot is known to be endothermic by about 0.3 eV due to electrostatic effects;[9] this process should not occur at room temperature as long as the capping layer remains intact. Energy transfer to a neighboring dot is resonant and not exothermic, but it is hard to imagine how it could be this fast unless there were a partial chemical bonding between the two dots, with loss of capping molecules in between.

In the case of very small interdot spacings, with only partial pyridine capping in pyridine arrays, rapid electron or hole tunneling can be considered a possible cause of our exciton absorption observations. Rapid electron and/or hole coupling between neighboring dots through the organic ligands capping the respective particles, could lead to a decrease in the electron and/or hole confinement energy in Eq. (1). This could occur by quantum mechanical tunneling through the barriers provided by the organic capping molecules on adjacent dots or by thermal excitation and subsequent hopping above these barriers, as in thermionic emission. Such tunneling could account for the decrease of the band gap energy with pressure relative to the observed energies for isolated dots. Concomitantly, this decreased lifetime would account for the broadened exciton width. If interdot coupling increases as the dots get closer—with no concomitant change in barrier height—the coupling would be due to tunneling rather than thermal hopping.

a. Band alignment. Interdot tunneling depends on the barriers seen by electrons and holes and the interdot distance, which depend on pressure. The interdot energy level structure is determined by the capping molecules and other possible barriers, such as that due to oxidation at the surface. Figure 8(a) shows the bands in CdSe and levels in pyridine assuming alignment of the vacuum levels. The top of the valence band and bottom of the conduction band in CdSe are shown for bulk CdSe (dashed lines), and the lowest hole and electron confined states are shown for the CdSe nanocrystal. With alignment of the vacuum levels there appears to be no barrier for electrons to go from CdSe to the lowest unoccupied molecular orbital of pyridine, and there is a large barrier for holes to go to the highest occupied molecular orbital of the pyridine. This would suggest that electron tunneling from dot to dot would see only the barrier between the pyridine ligands on nearest-neighbor dots. The band alignment will be different after the transfer of electrons associated with pyridine bonding to the CdSe nanocrystal, with a decrease in the hole barrier and possibly the formation of an electron barrier. Interdot tunneling through resonant pyridine states is possible and it could change with pressure; it is difficult to assess its importance. Figure 8(b) depicts the alignment of bulk bands of CdSe (core) with either CdS, ZnSe, or ZnS (shell) at a bulk planar interface[14,15,35,36] (which is discussed further later). When coupled with Fig. 8(a), this figure gives the barrers for interdot carrier tunneling between core/shell dots. Given the uncertainties in the energy level diagrams in Fig.

Downloaded 26 Jul 2002 to 128.59.115.125. Redistribution subject to AIP license or copyright, see http://ojps.aip.org/japo/japcr.jsp

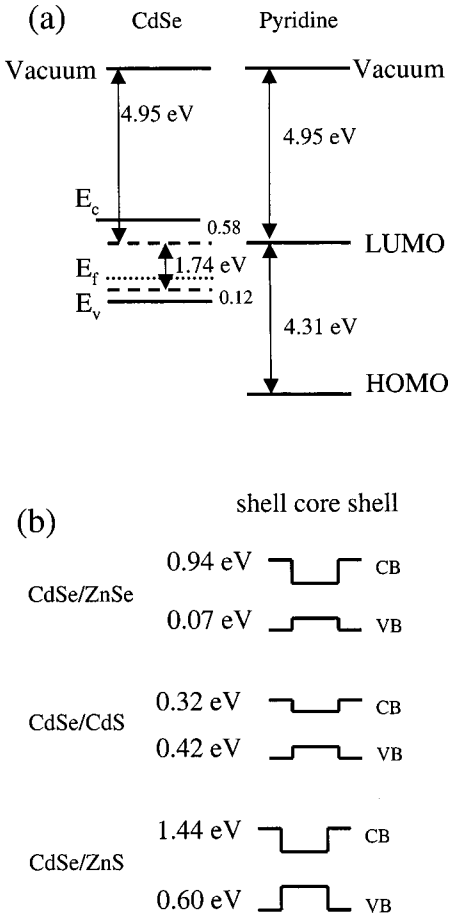

FIG. 8. (a) Band alignment of CdSe/pyridine assuming the lineup of vacuum levels. (b) Band alignments of the core/shell systems assuming no strain, with listed band offsets (see Refs. 35 and 36).

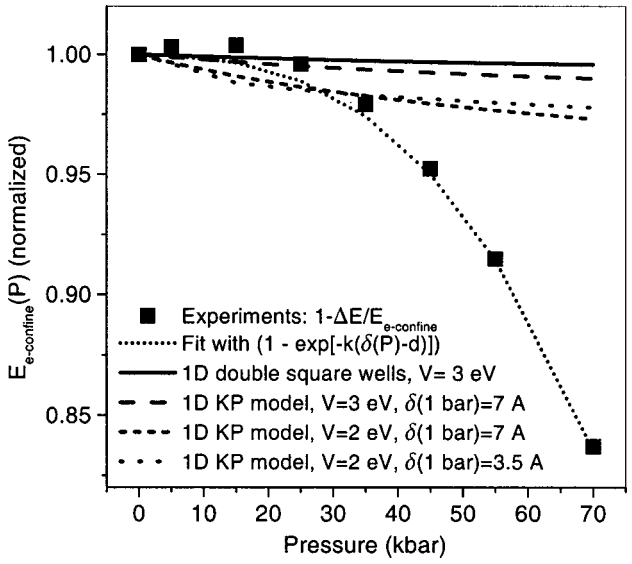

FIG. 9. Tunneling models, two coupled 1D square wells and 1D Kronig–Penney models, with various barrier heights are shown. In the Kronig–Penney models the electron masses are 0.12 m_e, the electron effective mass of CdSe, in the wells and m_e in the barriers. Also plotted are the deviations of experimental first exciton absorption peak energies for the CdSe/pyridine run denoted by asterisks in Fig. 5 from the solid line fit in Fig. 2(b). The normalized experimental data are well fit by $1-\exp\{-k[\delta(P)-d]\}$, with $d=4.8$ Å and $k=3.42$ Å^{-1} for $\delta(1\text{ bar})=7$ Å, and $d=2.4$ Å and $k=6.85$ Å^{-1} with $\delta(1\text{ bar})=3.5$ Å. The variation of barrier width (= interdot spacing) $\delta(P)$ with pressure is from the case of solid benzyl between the dots in Fig. 10. All energies are normalized by the electron confinement energy 560 meV.

8, the interdot tunneling model used here assumes square barriers of variable height between the nanoparticles.

b. Model. The results of model calculations for ground-state confinement energy changes expected by quantum mechanical tunneling are shown in Fig. 9. These are based on models of two coupled one-dimensional (1D) square wells and a 1D Kronig–Penney model of an infinite series of such coupled wells to determine the ground state of the system. In each case the barrier is of constant height V and the well separation is δ. In these calculations, V is not assumed to vary with pressure, while the separation between dots δ varies with pressure. This variation is shown in Fig. 10, and is described in the Appendix.

Electron tunneling is assumed in Fig. 9, and the electron confinement energies are plotted normalized to the electron confinement energy at ambient pressure (560 meV). Results are plotted for barriers of 2 and 3 eV, assuming electron masses of 0.12 m_e (the effective mass in bulk CdSe) in the wells and the free electron mass m_e in the barriers. The interdot separation at 1 bar is taken to be either 7 Å, that for either pyridine or TBPO capping—and which corresponds to about two molecules separating nearest neighbor dots—or 3.5 Å, which would correspond to about one molecule separating neighboring dots. (The reason for this is given later.) While this simplified analysis does not include cluster shape effects[18] or the exciton fine structure, it should semiquantitatively predict confinement energy changes. Note that the fractional changes in confinement energy in these 1D models and symmetric 3D cases are the same.

Also plotted in Fig. 9 are the deviation of the experimental first exciton absorption peaks for the CdSe/pyridine run denoted by asterisks in Fig. 5 from the solid line fit from Fig. 2(b), normalized by the electron confinement energy at 1 bar. The experimental results are larger in magnitude than those

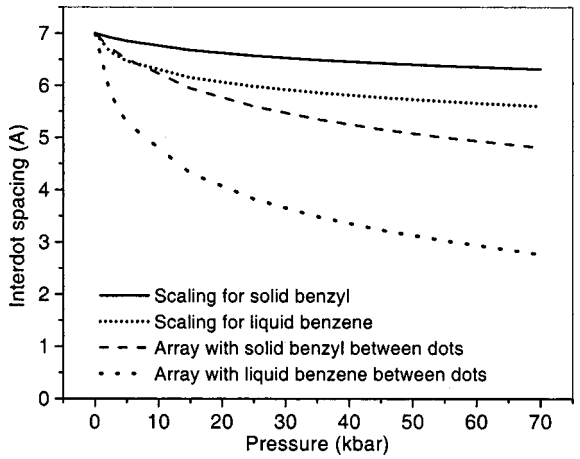

FIG. 10. Interdot separation as a function of pressure modeling the interdot medium as either solid benzyl or liquid benzene, as described in the Appendix. Also shown is how a length of 7 Å in these two media scales with pressure in the bulk. (Any phase transition in the liquid benzene is not included in these models.)

Downloaded 26 Jul 2002 to 128.59.115.125. Redistribution subject to AIP license or copyright, see http://ojps.aip.org/japo/japcr.jsp

of the model for the relatively small barriers and smaller interdot separations at ambient pressure. Moreover, the shape of the experimental and model pressure dependences are very different.

The normalized experimental data are well fit by the fit $1-\exp\{-k[\delta(P)-d]\}$, with $d=4.8$ Å and $k=3.42$ Å^{-1} for $\delta(1\text{ bar})=7$ Å, and $d=2.4$ Å and $k=6.85$ Å^{-1} with $\delta(1\text{ bar})=3.5$ Å—and with $\delta(P)$ varying as the case of solid benzyl between the dots in Fig. 10. k is a fitting parameter that has the form expected for tunneling with a critical distance of d. This is a phenomenological fit, which is less grounded in theory.

c. Assessing the importance of array periodicity. The distances from a dot to the six nearest-neighbor dots should be the same for a perfect array, and these distances should decrease by the same fraction with increased pressure. For the corresponding six pairs of dots in a glassy array, some of these interdot distances will be the same as in the close-packed perfect array at each pressure, and some will be larger. Much of the confinement energy for either carrier is lost by the interaction of two neighboring dots—say two nearest neighbors in an amorphous array. This can be seen by the generalization of the confinement term in Eq. (1) to spheroids of semiminor radius a and semimajor radius b:[12]

$$E_e=\frac{\pi^2\hbar^2}{2m_e(a^2b)^{2/3}}$$

The confinement energy decreases by 37% from an isolated sphere $b=a$ to two merged spheres of radius a approximated by a spheroid with $b=2a$. Consequently, similar strong evidence of interdot coupling could be expected from either completely ordered 3D arrays or from thoroughly dried amorphous arrays.

d. Summary. While the phenomenological fit agrees with observations, the Kronig–Penney quantum mechanical models of interdot carrier tunneling do not.

2. Implications of the core/shell nanocrystal results

The use of core/shell nanocrystals can provide a test of the tunneling hypothesis precisely because the shell can decrease the magnitudes of the electron and/or hole wave functions at the outer semiconductor surface and lessen the probability of interdot coupling.

Figure 8(b) depicts the alignment of bulk bands of CdSe (core) with either CdS, ZnSe, or ZnS (shell) at a bulk planar interface using calculated valence band offsets and assuming no strain.[14,15,35,36] Given the ~560 meV confinement energy of electrons and ~120 meV confinement energy of holes in core-only dots, this suggests that a CdS shell is a small barrier for holes and no barrier for electrons, a ZnSe shell is a big barrier for electrons and no barrier for holes, and a ZnS shell is a barrier for both electrons and holes. The hole confinement properties of CdS and ZnS shells and the completeness of the shells seem to be proven by the very strong luminescence of CdSe/CdS and CdSe/ZnS core/shell particles, even with pyridine capping. Still, there are definite uncertainties about these band alignments, aside from the inclusion of strain. For example, most calculations suggest that the CdSe/CdS interface has type I band alignment, as shown in Fig. 8(b). Reference 37 suggests it has type II alignment. However, what is more significant here is that all of the calculations suggest the CdS shell causes the confinement of holes in the CdSe core.

The application of pressure could potentially change the magnitude and signs of these band offsets. Reference 38 shows that the band gap of ZnS increases faster with P ($\alpha=6.4\times10^{-3}$ eV/kbar) than that of CdSe. The calculations in Ref. 39 suggest that this is true, and that both the conduction and valence band offsets at the CdSe/ZnS interface increase with P (with the relative change of the conduction band offset being larger than that of the valence band). This suggests that the confinement of electrons and holes would increase within the core in CdSe/ZnS dots as pressure increases.

The similar anomalous change in absorption exciton energy versus P for arrays of CdSe/pyridine and CdSe/CdS/pyridine in Figs. 5 and 6 would suggest that any observable tunneling would be by electrons and not by holes. However, similar observations are also seen for CdSe/ZnS/pyridine arrays. The band alignment for planar CdSe/ZnS interfaces suggests that the larger-band gap ZnS shell provides a barrier for electrons and holes, which would greatly decrease the interdot tunneling by either carrier.

The PL peak energy versus P traces for the CdSe/shell/pyridine arrays in Fig. 6(a) are approximately the same as those for the solution runs [in Fig. 2(a)]. Since the loss of pyridine on the outer surface of the semiconductor is approximately the same for the core-only and core-shell quantum dots, this would imply that there is no significant deviation from hydrostatic behavior, unless any such local nonhydrostaticity leads to PL quenching locally.

Overall, the core-shell dot results cast doubt on the tunnelling mechanism.

3. Energy transfer

Long-range energy transfer between CdSe dots by dipole–dipole coupling[7,8] could also be a factor in the CdSe/pyridine array results. This has been observed in array of CdSe/TOPO nanoparticles.[7,8] However, such dipole–dipole coupling does not influence the absorption spectra.[7,8] Also, since no PL is seen from CdSe/pyridine, the nonradiative lifetime is so fast that dipole–dipole coupling is unlikely to be important in interdot coupling.[7,8]

4. Contact between particles

The CdSe/pyridine array results could also arise from the contact between bare nanoparticles, with consequently less carrier confinement energy and nonhydrostaticity in pressure. This could lead to the fusion of nearest-neighbor nanoparticles into larger particles. Such fusion would be expected to be irreversible. However, in most runs the peaks during the pressure downstroke matched those during the upstroke, which would argue against clumping. Nonhydrostatic effects could occur between bare particles without fusion, as with powder media; however, it is expected that loading by liquid Ar would lessen this effect, with Ar flowing into the interstitial regions. Still, this is not definitive proof that bare sur-

Downloaded 26 Jul 2002 to 128.59.115.125. Redistribution subject to AIP license or copyright, see http://ojps.aip.org/japo/japcr.jsp

faces are not in contact and the possibility of contact of the semiconductor cores needs to be considered further. Note that any sort of inhomogeneity in conditions, such as in spatial variations in properties such as pressure, could lead to the observed broadening and shifts.

The pyridine capping molecules are much more weakly bound to the surface than are TOPO or TBPO. It is possible that if surface-bound pyridine leaves the dot surface, neighboring CdSe/pyridine could come into contact at high pressure. Recently, the authors followed these pyridine ligands during the drying of CdSe/pyridine dots in pyridine solution on a ZnSe element in a Fourier-transform infrared spectrometer by using ATR spectroscopy.[40] The inset to Fig. 7 shows the ATR spectrum of a ~1-μm-thick array of CdSe/pyridine after the solvent has evaporated; in these thick films the pyridine solvent evaporates in 20–30 min. The main part of the figure follows the 1445 cm^{-1} peak of bound pyridine as a function of drying time. For these thick films, which approximate the thickness of those used in this study, much of the initial pyridine capping was lost during the typical 3 day drying time, but about 30%±8% remained.[40] Pyridine ligands were seen to leave thinner films faster than from thicker films, so more loss of pyridine capping is expected from the top of the film than from the bottom. In Fig. 7 it is seen that pyridine leave the outer surfaces of the ZnS shell in CdSe/ZnS dots, where pyridine likely binds to the Zn sites, at about the same rate as for CdSe core dots.

The bare CdSe surfaces of a pair of nearest-neighbor dots can touch when they both lack organic ligands locally in the contact region. The probability of this occurring is estimated with a statistical model that assumes that the dots are spherical (which is not rigorously true), the adsorption sites form a quasisquare lattice on the sphere (which is not rigorously true), and the pyridine molecules desorb from random positions on the dot (which may be reasonable). There are about 200 surface atoms on the surface of these 3.3 nm diameter CdSe dots, approximately 100 Cd and 100 Se atoms. In the synthesized CdSe/TOPO nanoparticles all of these Cd sites are thought to be capped, ~70% by TOPO and ~30% by TOPSe.[41] Another study suggests that only TOPO, and not TOP, binds to the nanocrystal surface.[13] Refluxing in pyridine removes about 85%–90% of the TOPO.[14,23,40] Pyridine is thought to bind only to the Cd sites.[13] It is assumed that all of the 100 Cd sites are terminated by a molecule initially (for now let us say only pyridine), and that after drying a fraction x of the sites remain capped. A geometrical model shows that nearest-neighbor dots can (usually) touch at bare CdSe regions if each of the eight Cd sites in the overlapping 2×2 square arrays of Cd sites on neighboring dots are not capped by pyridine (Fig. 11). This probability is $y=(1-x)^8$. Even when this occurs, the dots do not touch if there is a pyridine molecule both in any one of the eight nearest-neighbor sites surrounding the 2×2 square array on one dot and the corresponding site on the other dot (Fig. 11). The probability that this occurs is $z=1-(1-x^2)^8$. With six nearest-neighbor dots surrounding each dot, the probability that a given dot will touch a neighbor is $1-[1-y(1-z)]^6$. For $x=0.25$, 0.30, 0.35, and 0.40 these probabilities are 30.9%, 15.2%, 6.5%, and 2.5% respectively. In a disordered array, there are fewer than six ''nearest''-neighbor dots and this probability is smaller. ATR tracks the fraction of pyridine ligands that remain (~30%±8%). Still about 10% of the surface sites are still bound by the larger TOPO, even after exchange with pyridine.[14,23,40] This also decreases the probability of contact. Even with the crudeness of this model, it is clear that contacting of bare particle sites in the CdSe/pyridine cannot be ignored if only ~30% of the capping pyridine molecules remain.

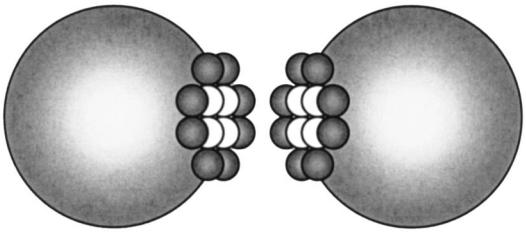

FIG. 11. Schematic of those pyridine sites on neighboring dots that can be involved in contact between the dots, including the four (2×2) inner sites (white) and eight surrounding ones (gray) on each dot described in the model. (Not drawn to scale.)

With fewer capping ligands, the distance between neighboring dots is smaller (at ambient pressure and at higher pressures), even with no contact. The interdot separation of CdSe/pyridine is likely much less than 7 Å at ambient pressure. If tunneling occurs between the dots it could be across one (or no) pyridine molecules, instead of the two expected if there pyridine ligands at each site. This is why the case of an ambient pressure separation of 3.5 Å was also analyzed in Fig. 9.

The ATR results[40] suggest that in the CdSe/pyridine arrays dried for 1–2.5 h about 70%±10% of the surface pyridine remains after drying and there is essentially no pyridine solvent remaining. The similarity of the high pressure results for such arrays and those of Fig. 2(b) may mean that there is no interdot coupling through the two pyridine molecules spacing adjacent dots. In the arrays dried for 6 and 14 days, there is an estimated 16% and 13% capping by pyridine, respectively (in addition to the residual TOPO). The large hysteresis seen in these runs may indicate that there is dot contact and that this contact is irreversible when the pressure is lowered, i.e., clumping. It could mean that in the Fig. 5 runs with 3 days of drying there is particle contact at higher pressure that is reversible or there is interdot tunnelling and no contact.

Terms 3 and 4 in Eq. (1) should be sensitive to partial contact between particles at ~50 kbar, and could account for the changes seen in absorption. Pyridine is more volatile than TOPO, and leaves the arrays under pronounced drying. Following long drying at elevated temperature, the high pressure data develops hysteresis, which suggests that compression creates partial bonding between particles. If the local dielectric neighborhood contains more CdSe and less pyridine, then term 4 will become less positive, and the Coulomb energy will increase towards its value in pure CdSe. This possibility is quantitatively considered in the next section.

Overall, the possibility of significant interdot contact cannot be excluded. It could be responsible for the unusual

Downloaded 26 Jul 2002 to 128.59.115.125. Redistribution subject to AIP license or copyright, see http://ojps.aip.org/japo/japcr.jsp

observations for CdSe/pyridine arrays at high pressure.

5. Changes in the surrounding dielectric medium

A possible cause of the CdSe/pyridine results is the change with pressure in the organic dielectric medium, in the fourth term of Eq. (1). At ambient pressure, the first exciton peak occurs at the same energy in CdSe/TOPO in solution and in arrays, as was earlier seen by Kagan *et al.*[8] In contrast, the first exciton absorption peak at 1 bar occurs at 24 meV lower energy for the dried CdSe/pyridine arrays than in solution (Fig. 3). This shift might be explained by the different dielectric environment in the arrays. By using the volume-averaged dielectric constant of 4.6 of the fcc structure of dot arrays and inter-CdSe dot pyridine (using the high frequency $\epsilon = 7.74$ for CdSe[42] and 2.28 for pyridine,[43] and the model for the relative volumes of CdSe and pyridine from the Appendix), term 4 predicts a shift of 26.7 meV to lower energy in the arrays (from 47.5 meV in pyridine solution to 20.8 meV in the array), which is consistent with observations. If only 35% of the pyridine ligands remain and there are no voids, then a larger shift of 37.6 eV to lower energy (to 9.9 meV) would occur.

As pressure is increased, the solvation energy term predicts a further decrease in the energy of the exciton absorption peak. The changes in the dot radius and relative volumes of the semiconductor and organic phases are given by Murnaghan's equation and the Appendix (solid benzyl model). The increase in the dielectric constant of the organics with pressure is slower than the decrease in volume;[44] it is estimated to increase by a factor of 1.5 from 1 bar to 50 kbar. The CdSe dielectric constant is assumed not to change because of the relatively small decrease in CdSe volume. Term 4 in the dilute solution of 47.5 meV at 1 bar becomes 48.9, 32.2, and 33.1 meV at 50 kbar when, respectively, including the changes in dot radius only, organic dielectric constant only, and both effects. In the array it is 20.8 meV at 1 bar and becomes 19.3 and 14.3 meV (15.7 and 11.8 meV for the Tait model in the Appendix) at 50 kbar when, respectively, including the changes in dot radius and volume fraction only, and these plus the organic dielectric constant change. (The decrease of R with P causes term 3 in Eq. (1) to decrease by 6.3 meV for both dilute solutions and arrays.) So, the difference in this term between the solution and array goes from 26.7 meV at 1 bar to 29.6 and 18.8 meV (33.2 and 21.3 meV) at 50 kbar, when including, respectively, only radius and volume changes, and then also dielectric constant changes of the organic. The changes of dot radius and relative volume with pressure increase the difference by 2.9 meV (6.5 meV), much less than that observed; when the dielectric constant of only the organic is also included, the difference actually decreases with pressure. This change in the surrounding dielectric medium with P does not seem to be significant here.

6. Further discussion

Artemyev *et al.*[10] observed that at ambient pressure the CdSe/pyridine absorption exciton peaks are much broader for arrays than for structures with dispersed CdSe/pyridine nanoparticles (in polymer hosts, etc.), which suggested interdot coupling. No such broadening is seen here. The absorption spectrum of the nanoparticles in highly dried arrays and solutions are the same, aside from the dielectric shift in Fig. 3.

The probability of charge separation and collection in CdSe dot solids is apparently very small, as measured by photoconductivity.[9] At high electric fields (250 kV/cm) fewer than 1×10^{-4} charges are collected per photon. The energy needed to separate an electron-hole pair in a given 3 nm diameter CdSe dot to produce an electron and hole in neighboring dots is calculated to be ~ 0.3 eV for carriers confined to the core and ~ 0.1 eV for carriers trapped on the surface.[9] Such separation energies would be expected to decrease with pressure because of the smaller separation between the dots and the increased dielectric constant of the interdot medium. These energy barriers would also be important in the current study unless the exciton itself can tunnel from dot-to-dot. Exciton tunneling (which is distinct from radiative transfer) would also lower the carrier confinement energy; it cannot be sensed in photoconductivity and also may be improbable. At low applied electric fields the photocurrent is larger by an order of magnitude for CdSe/TBPO and CdSe/pyridine than in CdSe/TOPO solids. This is due to the smaller interdot separation in the former systems and is consistent with tunneling through alkanethiols, which occurs with a probability of $\sim\exp(-\delta/D)$ where $D\sim 1.2$ Å.[45] If D does not vary with pressure, this relationship suggests that changing the interdot distance from 7 to 5 or 3 Å will increase the probability of tunneling by ~ 5 or 30. Coating CdSe/pyridine by three monolayers of ZnS decreases the collected charge per photon by at least a factor of 160, due to the large energy barrier for the carriers. Similarly, one would expect that interdot coupling as sought here would be decreased greatly by such ZnS shells.

In summary, the CdSe/ZnS/pyridine array experiments suggest that the unusual absorption measurements at high pressure in CdSe/pyridine arrays cannot be attributed to carrier coupling. The importance of contact of the semiconductor surfaces of neighboring dots cannot be excluded.

V. CONCLUDING REMARKS

The PL and absorption spectra of solutions and arrays of CdSe/TOPO or TBPO nanocrystals are the same up to 60 kbar. Consequently, they exhibit no evidence of interdot coupling. In each of these systems, the variation with pressure is roughly that expected from the increase in band gap energy of bulk CdSe with pressure and the increase in confinement energies of electrons and holes with increased pressure, which results from the smaller dot dimensions. However, the difference in the energy of the PL peak and the first exciton in absorption for these solutions and arrays increases with pressure. The observed large increase in this Stokes shift with pressure is attributed mostly to an increased vibrational Stokes shift. In contrast, there is a distinct difference between the pressure dependence of isolated and arrays of CdSe/pyridine. While the pressure dependence of the first exciton in absorption in isolated CdSe/pyridine looks the

Downloaded 26 Jul 2002 to 128.59.115.125. Redistribution subject to AIP license or copyright, see http://ojps.aip.org/japo/japcr.jsp

same as that in all runs with CdSe/TOPO and CdSe/TBPO, the increase of exciton energy with pressure becomes markedly slower above about 30 kbar in CdSe/pyridine arrays. Since no PL could be observed from the pyridine-capped particles, this was only observed in absorption. This different dependence could be attributed to several factors: (1) rapid electron and/or hole coupling between neighboring nanoparticles through the organic ligands capping the respective particles leading to a decrease in electron and/or hole confinement energy, (2) nanoparticle nanoparticle contact, (3) fusion of nearest-neighbor nanoparticles into larger particles, and/or (4) nonhydrostatic pressure conditions. Several experimental observations suggest the last two factors are not important. Experiments with CdSe/shell dots, with large electron and hole barriers, cast doubt on the tunneling mechanism. The energy required for separating charges from one dot to neighboring dots decreases with pressure, but may still be significant. The differences in the dielectric medium surrounding each dot in the solution and array explain differences in absorption exciton energies at 1 bar, but not these changes at high pressure. The loss of much of the pyridine ligands during array drying could be very significant and contact between dots may be important.

ACKNOWLEDGMENTS

This work was supported by the Materials Research Science and Engineering Center under Grant No. DMR-98-09687 and the Joint Services Electronics Program DAAG055-97-1-0166. The authors would like to thank C. B. Murray, A. P. Alivisatos, U. Banin, A. Efros, M. Bawendi, and M. Newton for valuable discussions and suggestions.

APPENDIX

At ambient pressure, it is thought that the medium between the dots in the array is filled by the capping molecules.[12] This is assumed to be so in Fig. 10, where the interdot spacing is determined by following the volume of interdot material versus P for fcc closest-packed spheres with a packing density of 0.74. For spheres of radius $R+\delta/2$ (R for the semiconductor and $\delta/2$ for the capping molecules for an interdot separation of δ), the volume of organic ligand is $V=V_1$ (that on the dot) + V_2 (that in between the dots) per dot, where $V_1=4\pi[(R+\delta/2)^3-R^3]/3$ and $V_2=4\pi(R+\delta/2)^3[1/0.74-1]/3$.

The interdot spacing is estimated by following the volume of the organic medium using either Murnaghan's equation of state—often used for solids[46]

$$\frac{V(P)}{V(1\ \text{bar})}=\left(1+\frac{B'}{B}P\right)^{-1/B'},$$

where B is the bulk modulus and $B'=dB/dP$, or the Tait equation of state—often used for liquids[47]

$$\frac{V(P)}{V(1\ \text{bar})}=\left[1-c\ln\frac{(b+P)}{(b+P_0)}\right],$$

where c and b are parameters. P_0 is the ambient pressure, 1 bar. This variation of V with pressure gives $\delta(P)$ for a given $R(P)$. This change in the core CdSe radius can be determined from Murnaghan's equation, and is small enough to be ignored here. Equation of state parameters are not available for the ligands of interest. For pyridine, parameters $B=61.26$ kbar and $B'=7.168$ for solid benzyl,[48] and $c=0.111$ and $b=0.874$ kbar[49] for liquid benzene were used. This gives $\delta(P)$, which is plotted in Fig. 10; it is used in the model of the confinement energy. If the medium between the dots in the array is not filled entirely by the capping molecules, δ decreases even faster with P. The assumption of a liquid phase is valid only up to the phase transition to the solid phase. Moreover, there is great uncertainty in using equations of state designed for bulk materials for essentially single layers of organic molecules. Also plotted in Fig. 10 for reference is the corresponding change in linear dimensions in pure bulk solid benzyl and liquid benzene at elevated pressure.

The results of this model are used in the tunneling calculations shown in Fig. 9.

[1] Al. L. Efros and A. L. Efros, Fiz. Tekh. Poluprovodn. (S.-Petersburg) **16**, 1209 (1982) [Sov. Phys. Semicond. **16**, 772 (1982)].
[2] L. E. Brus, J. Chem. Phys. **80**, 4403 (1984).
[3] L. Brus, Appl. Phys. A: Mater. Sci. Process. **53**, 465 (1991).
[4] C. P. Collier, R. J. Saykally, J. J. Shiang, S. E. Henrichs, and J. R. Heath, Science **277**, 1978 (1997).
[5] G. Markovich, C. P. Coller, and J. R. Heath, Phys. Rev. Lett. **80**, 3807 (1998).
[6] G. Medeiros-Ribeiro, D. A. A. Ohlberg, R. S. Williams, and J. R. Heath, Phys. Rev. B **59**, 1633 (1999).
[7] C. R. Kagan, C. B. Murray, M. Nirmal, and M. G. Bawendi, Phys. Rev. Lett. **76**, 1517 (1996).
[8] C. R. Kagan, C. B. Murray, and M. G. Bawendi, Phys. Rev. B **54**, 8633 (1996).
[9] C. A. Leatherdale, C. R. Kagan, N. Y. Morgan, S. A. Empedocles, M. A. Kastner, and M. G. Bawendi, Phys. Rev. B **62**, 2669 (2000).
[10] M. V. Artemyev, A. I. Bibik, L. I. Gurinovich, and S. V. Gaponenko, Phys. Rev. B **60**, 1504 (1999).
[11] C. B. Murray, C. R. Kagan, and M. G. Bawendi, Science **270**, 1335 (1995).
[12] C. B. Murray, Doctoral thesis, MIT, 1995.
[13] P. Guyot-Sionnest, M. Shim, C. Matranga, and M. Hines, Phys. Rev. B **60**, R2181 (1999).
[14] X. Peng, M. C. Schlamp, A. V. Kadavanich, and A. P. Alivisatos, J. Am. Chem. Soc. **119**, 7019 (1997).
[15] B. O. Dabbousi, J. Rodriguez Viejo, F. V. Mikulec, J. R. Heine, H. Mattoussi, R. Ober, K. F. Jensen, and M. G. Bawendi, J. Phys. Chem. B **101**, 9463 (1997).
[16] M. Danek, K. F. Jensen, C. B. Murray, and M. G. Bawendi, Chem. Mater. **8**, 173 (1996).
[17] D. J. Norris and M. G. Bawendi, J. Chem. Phys. **103**, 5260 (1995).
[18] X. G. Peng, L. Manna, W. D. Yang, J. Wickham, E. Scher, A. Kadavanich, and A. P. Alivisatos, Nature (London) **404**, 6773 (2000).
[19] C. B. Murray, D. J. Norris, and M. G. Bawendi, J. Am. Chem. Soc. **115**, 8706 (1993).
[20] S. H. Tolbert and A. P. Alivisatos, Science **265**, 373 (1994).
[21] S. H. Tolbert and A. P. Alivisatos, J. Chem. Phys. **102**, 4642 (1995).
[22] H. Mattoussi, A. W. Cumming, C. B. Murray, M. G. Bawendi, and R. Ober, Phys. Rev. B **58**, 7850 (1998).
[23] M. Kuno, J. K. Lee, B. O. Dabbousi, F. V. Milkulec, and M. G. Bawendi, J. Chem. Phys. **106**, 9869 (1997).
[24] C. R. Kagan, Doctoral thesis, MIT, 1996.
[25] C. B. Murray (private communication).
[26] J. Schroeder and P. D. Persans, J. Lumin. **70**, 69 (1996).
[27] J. R. Mei and V. Lemos, Solid State Commun. **52**, 785 (1984).
[28] H. X. Fu, L. W. Wang, and A. Zunger, Phys. Rev. B **59**, 5568 (1999).
[29] Al. L. Efros, M. Rosen, M. Kuno, M. Nirmal, D. J. Norris, and M. Bawendi, Phys. Rev. B **54**, 4843 (1996).
[30] M. Nirmal, D. J. Norris, M. Kuno, and M. G. Bawendi, Phys. Rev. Lett. **75**, 3728 (1995).

Downloaded 26 Jul 2002 to 128.59.115.125. Redistribution subject to AIP license or copyright, see http://ojps.aip.org/japo/japcr.jsp

[31] P. Lefevbre, B. Gil, and H. Mathieu, Phys. Rev. B **35**, 5630 (1987).
[32] J. N. Wickham, A. B. Herhold, and A. P. Alivisatos, Phys. Rev. Lett. **84**, 923 (2000).
[33] R. Marcus, J. Chem. Phys. **24**, 966 (1956).
[34] V. I. Klimov, A. A. Mikhailovsky, D. W. McBrach, C. A. Leatherdale, and M. G. Bawendi, Phys. Rev. B **61**, R13349 (2000).
[35] S. H. Wei and A. Zunger, Appl. Phys. Lett. **72**, 2011 (1998).
[36] S. H. Wei, S. B. Zhang, and A. Zunger, J. Appl. Phys. **87**, 1304 (2000).
[37] S. Pokrant and K. B. Whaley, Eur. Phys. J. D **6**, 255 (1999).
[38] J. M. Lang, Z. A. Dreger, and H. G. Drickamer, J. Solid State Chem. **106**, 144 (1993).
[39] C. G. Van de Walle, Phys. Rev. B **39**, 1871 (1989).
[40] B. S. Kim, L. Avila, L. E. Brus, and I. P. Herman, Appl. Phys. Lett. **76**, 3715 (2000).
[41] L. R. Becerra, C. B. Murray, R. G. Griffin, and M. G. Bawendi, J. Chem. Phys. **100**, 3297 (1994).
[42] E. D. Palik, *Handbook of Optical Constants of Solid II* (Academic, New York, 1991).
[43] *Beilsteins Handbuch der Organischen Chemie*, 4th ed. (1950), Vol. 20, p. 2205.
[44] D. W. Brazier, and G. R. Freeman, Can. J. Chem. **47**, 893 (1969).
[45] R. H. Terrill *et al.*, J. Am. Chem. Soc. **117**, 12537 (1995).
[46] F. D. Murnaghan, Proc. Natl. Acad. Sci. U.S.A. **30**, 244 (1944).
[47] D. S. Tsyklis, *Dense Gases* (Khimiya, Moscow, 1976).
[48] S. N. Vaidya and G. C. Kennedy, J. Chem. Phys. **55**, 987 (1971).
[49] V. Ya. Maslennikova, M. B. Nikiforova, and A. N. Doklady, SSSR **273**, 871 (1983).

Downloaded 26 Jul 2002 to 128.59.115.125. Redistribution subject to AIP license or copyright, see http://ojps.aip.org/japo/japcr.jsp